ELSEVIER

Biophysical Chemistry 59 (1996) 139–153

Biophysical Chemistry

Monte Carlo study for fluctuation analysis of the in vitro motility driven by protein motors

Yasuhiro Imafuku [a], Yoko Y. Toyoshima [b], Katsuhisa Tawada [a,c,*]

[a] *Department of Molecular Biology, Graduate School of Medical Sciences, Kyushu University, Fukuoka 812, Japan*
[b] *Department of Pure and Applied Sciences, College of Arts and Sciences, University of Tokyo, Komaba, Tokyo 153, Japan*
[c] *Department of Biology, Faculty of Science, Kyushu University, Fukuoka 812, Japan*

Received 8 May 1995; revised 31 July 1995; accepted 28 September 1995

Abstract

The fluctuation properties of the sliding movement of an individual cytoskeletal filament driven by protein motors in vitro can be analyzed by calculating the mean-square deviation of the displacement from the average within its single trajectory. For this purpose, a Monte Carlo simulation was used to define the conditions and limitations of a method for smoothing (curved) noisy trajectories without affecting either the steady or fluctuation characteristics inherent to the individual filament sliding movement. By applying the method to real experimental trajectory data, we show that an effective diffusion coefficient from displacement fluctuations of a sliding filament can be obtained from its single noisy trajectory even when it is curved.

Keywords: Sliding movement; Cytoskeletal filaments; Random walk, biased; Diffusion; Monte Carlo study; Motility; Cell motility

1. Introduction

Protein motors cause a unidirectional sliding movement of cytoskeletal filaments in vitro. For example, myosin motors attached to a solid surface induce actin filaments to slide unidirectionally [1]. Either kinesin motors or dynein motors attached to glass surface induce microtubule filaments to slide [2,3]. The sliding filaments are subjected to various forces: the active force generated by the protein motors, drag forces opposing the directional sliding movement, which limit the sliding velocity [4,5], and random forces from the collision of thermally agitated solvent molecules as well as from the thermal motion of the protein structures of the motors [5].

The characteristics of the dominant forces involved in the sliding movement in vitro can be studied by analyzing the fluctuation of the movement. A key statistical quantity for the analysis is the mean-square deviation of the sliding displacement from the average. This mean-square deviation as a function of the time yields an effective "diffusion coefficient", which will be referred to as a motional diffusion coefficient, and the length dependence of the motional diffusion coefficient provides clues to elucidate the characteristics of the forces involved in

* Corresponding author. Correspondence address: Department of Biology, Faculty of Science 33, Kyushu University, Fukuoka, Fukuoka 812-81, Japan. Fax and Tel: (+81) 92 632 2742; E-mail: ktawascb@mbox.nc.kyushu-u.ac.jp.

SSDI 0301-4622(95)00123-9

the sliding movement in vitro, as will be explained below.

In thermally generated Brownian movements, the longitudinal diffusion coefficient of a filamentous particle is approximately inversely proportional to the filament length. Such an example of the Brownian movements has been reported by Vale et al. [6] with microtubules on a dynein-coated surface in the presence of vanadate (an inhibitor of dynein) and ATP. The inverse proportionality of the length dependence of the longitudinal diffusion coefficient is a direct consequence of the central limit theorem with the premise that the molecules which cause the Brownian movement of a filament interact with it at random [7].

The motional diffusion coefficient of a sliding cytoskeletal filament, which is defined above, is a measure of the fluctuation in the sliding movement, as is the diffusion coefficient in the Brownian movement. Examining the length dependence of the motional diffusion coefficient will therefore elucidate some characteristics concerning the randomness in the interaction of the protein motors with a sliding filament. Furthermore, we may be able to evaluate the coefficient of frictional drag imposed on a sliding filament [4,5] if the motional diffusion coefficient is found to be dependent upon the filament length, as we can do with the diffusion coefficient of a filamentous Brownian particle.

The mean-square displacement deviation from the average in the sliding movement is usually evaluated by averaging the sliding distances over a large collection of filaments with similar filament lengths. Consequently this averaging method does not provide a motional diffusion coefficient for each filament. For the filament length dependence study, however, it is necessary to obtain a motional diffusion coefficient for each individual filament. This can be done by the average calculation within a single trajectory of a filament. Qian et al. [8] discussed the theoretical basis of a single particle tracking method for particles undergoing either random diffusion or diffusion with drift, to obtain a diffusion coefficient for each individual particle.

In practice, the real sliding trajectories obtained by the conventional motility assay contain a relatively large amount of noise, which arise from the digitization of video images of filament positions with a mouse-driven cursor on a computer screen. The noise present in the trajectory data does not allow us to precisely determine the sliding distances along a single noisy, in particular curved, trajectory. It is thus difficult to calculate the mean-square displacement deviation from the average within a single trajectory, when it is noisy and curved. Calculating the centroid of a filament does not overcome this difficulty when the filament is long and flexibly curved, because it does not yield the accurate positions of such a filament and hence does not construct an accurate trajectory.

Using computer simulation, we have examined various methods for removing the digitization noise present in the position data of trajectories by data processing with a computer, in order to smooth over the trajectories without loosing any of the fluctuation and steady characteristics intrinsic to the sliding motion, and found that smoothing by the low-pass filtering of the trajectory data in a frequency domain worked successfully for the present purpose. Although there are limitations in the application of the present method, the method works for curved, as well as linear, noisy trajectories, consisting of a relatively small number of positional data points. This paper thus describes the results of a simulation study with an application to real experimental data. In separate studies, we will report more detailed results obtained by applying this method to the real experimental trajectories of the in vitro sliding movement of microtubule over either dynein or kinesin and of actin over myosin.

2. Methods

2.1. General protocol of the computer simulation study

(1) We consider that the sliding motion of a cytoskeletal filament driven by protein motors is a biased random walk [9]. To simulate this motion, we generate a one-dimensional biased random walk with a given average velocity and a given motional diffusion coefficient, using Monte Carlo simulation on a computer. We collect the positional data of a walk with a given sampling interval, which gives a set of

positional data of a particle as a function of discrete time. A set of time-series positional data forms a trajectory of a biased motion. From the positional data of a single trajectory, we then calculate the mean-square displacement deviation from the average. The mean-square deviation as a function of time yields an "experimental" value of the motional diffusion coefficient. The method for the mean-square deviation calculation will be given shortly.

(2) We next add random noise, as errors in digitizing the particle position, to the x- and y-axes coordinates of each discrete position datum of a trajectory. The characteristics of the type of noise will be explained shortly.

(3) We smooth the resulting noisy trajectory by "low-pass" filtering in the frequency domain (see below). From the discrete positional data in a smoothed trajectory, we then calculate the mean-square displacement deviation from the average as a function of time, and obtain an experimental value of the motional diffusion coefficient.

(4) We compare the "experimental" values of the motional diffusion coefficients obtained before adding digitization noise and after smoothing, with the original diffusion coefficient used for the simulation. We then examine the conditions for the low-pass filtering, under which the "experimental" diffusion coefficients obtained after the filtering are close to the original diffusion coefficients used for the simulation.

(5) We repeat the above four steps at various diffusion coefficients and average velocities.

2.2. *Generation of linear and curvilinear biased random walks in a two-dimensional plane*

We consider the motion of particles along a line. The particles start at time $t = 0$ at position $r = 0$, and execute a biased random walk. We apply the following rules for the random walk [10]:

(1) Each particle steps forward or backward along a line once every τ seconds, moving over a distance δ with a velocity of $\pm v_0$. Thus, $\delta = \pm v_0 \tau$. We treat τ and δ as constants for simplicity.

(2) The probability of going forward is p, and that of going backward is q $(= 1 - p)$. Successive steps are statistically independent.

The average displacement of a particle along a line after N steps is

$$\langle r \rangle = (p - q) N\delta \tag{1}$$

where $\langle r \rangle$ is calculated usually by averaging over many particles but here by averaging within a single trajectory of a particle (see below). The mean-square displacement deviation from the average (F_r^2), the variance of the displacement, is given by

$$F_r^2 = \langle (r - \langle r \rangle)^2 \rangle = 4pqN\delta^2 \tag{2}$$

$$= 4pq(\Delta t/\tau)\delta^2$$

$$= 2D_m \Delta t \tag{3}$$

where Δt is the time interval of N steps and D_m is the motional diffusion coefficient. So we have

$$D_m = 2pq\delta^2/\tau \tag{4}$$

On the other hand, $\langle r \rangle$ is proportional to the time interval Δt:

$$\langle r \rangle = \langle v \rangle \Delta t \tag{5}$$

where $\langle v \rangle$ is the average (drift) velocity of particles. From Eqs. 1–5, we obtain

$$p = (1 + \langle v \rangle / v_0)/2 \tag{6}$$

where $v_0 = (2D_m/\tau + \langle v \rangle^2)^{1/2}$.

Eq. 6 gives the probability for the forward step (p) in a biased random walk in terms of a given motional diffusion coefficient, a given drift velocity and a given value for τ. In this work, τ was fixed to be 1/900 s. With values for p calculated by Eq. 6, we generated one-dimensional biased random walks using Monte Carlo simulation, and collected the positional data with a sampling interval of 1/30 or 1/10 s. The sampling interval for digitizing the position of sliding filaments in real experiments, which should be as small as possible, is set to be large enough so as to be able to track the forward movement. In other words, the interval is set so that the position of a walker sampled at a time does not go back beyond the previous position along a trajectory. From our experience, we know that a sampling interval of 1/30 s is appropriate for actin/skeletal myosin and microtubule/dynein motility in vitro. A sampling interval of 1/10 s is appropriate for microtubule/kinesin motility in vitro.

For straight linear random walks in a two-dimen-

sional plane, positional increments in the x- and y-axes coordinates of a particle are given by

$$\mathrm{d}x(t_j) = \mathrm{d}r(t_j)\cos\Theta \tag{7}$$

and

$$\mathrm{d}y(t_j) = \mathrm{d}r(t_j)\sin\Theta \tag{8}$$

where $\mathrm{d}r(t_j)$ is the displacement of a particle along a track between the jth and $(j+1)$th sampling intervals and Θ was fixed at 45° for straight linear random walks, except where otherwise stated.

For curvilinear random walks in a plane, we varied Θ in Eqs. 7 and 8 as a function of sampling time (t_j) as

$$\Theta = \Theta(t_j) \tag{9}$$

The explicit form of $\Theta(t_j)$ will be given later.

The x-coordinate of the net displacement of a particle along a biased random walk track after n sampling intervals (= at the time of $n \times$ sampling intervals) is given by

$$x(t_n) = \sum_{j=1}^{n} \mathrm{d}x(t_j) \tag{10}$$

and its y-coordinate is given by

$$y(t_n) = \sum_{j=1}^{n} \mathrm{d}y(t_j) \tag{11}$$

2.3. Addition of digitization noise to the x- and y-coordinate data

In real experiments, various types of noise are introduced in the position measurement of the sliding filaments. There are two possible sources for the noise. One is the digitization process of the filament position on a computer screen, which introduces noise because of the discreteness of the pixel sites on the screen. The other is the uncertainty in reading the position marker (such as the filament tip) of video images of the sliding filaments on the screen. Such noise is random and is not correlated with time [8]. To simulate the noise introduction in experimental position measurements, we added random errors to the x- and y-coordinate values of the positional data generated by simulation as follows. The type and size of the random errors for the noise simulation were chosen so that the variance of the resulting positional errors (see $\sigma_{\epsilon x}^2$ in Eq. 18) is consistent with that obtained in real experiments.

On an imaginary screen, we plotted the discrete positional data points of a trajectory generated by a computer simulation for a biased random walk. On the screen, we overlaid a lattice, in which the lattice sites correspond to the pixel sites on a computer screen. Each of the discrete points of a random walk trajectory was then moved to the nearest-neighbor lattice sites so as to "digitize" the original data. As an uncertainty error in reading positions, we furthermore added random discrete errors to the x- and y-coordinates of each digitized positional datum: $n\epsilon_x$ and $n\epsilon_y$, in which n was a random integer (see below), with $\epsilon_x = 157$ nm and $\epsilon_y = 138$ nm corresponding to the distances between two adjacent pixels along the x- and y-axes on the computer screen under our real experimental conditions. The above n was given by a Gaussian random integer generator with a variance of 1 and an average of 0; n was thus one of the integers approximately in the range between -3 and $+3$ with a most probable value of 0.

2.4. Smoothing over of noisy trajectories

The time-series data of x- or y-coordinate, which were made noisy as described above, were smoothed in a frequency domain by low-pass filtering using fast Fourier transformation (FFT) and inverse fast Fourier transformation (IFFT) [11], to obtain smoothed trajectories. In short, (i) we first removed any linear trend from a set of time-series data of x- or y-coordinate, and low-pass filtered the Fourier components which were obtained by FFT of the resulting time-series data, and (ii) we then reconstructed a smooth trajectory, by IFFT followed by the reinsertion of the linear trend. In the original program for smoothing given by Press et al. [11], the Welch window is used for filtering in the frequency domain, but we found that the Hanning window [11] is more efficient for our purpose and used the latter window throughout the present study.

2.5. Calculation of the net displacement along a trajectory

The displacement of a particle along a trajectory in a time interval between t_j and t_{j+k} ($\Delta t = t_{j+k} -$

t_j) was calculated by one of the following two methods.

(1) Under the assumption that a trajectory is linear, the displacement is given by the distance between the two end points along the trajectory as

$$r(\Delta t) = \sqrt{\left[x(\Delta t)^2 + y(\Delta t)^2 \right]} \quad (12)$$

where $x(\Delta t) = x(t_{j+k}) - x(t_j)$ and $y(\Delta t) = y(t_{j+k}) - y(t_j)$. The distance thus calculated will be referred to as the linear distance between the two end points.

(2) The net displacement is given by the contour length along a trajectory. Noisy trajectories were first smoothed. To obtain the contour length, we summed up each distance between two adjacent points consecutively along a trajectory as

$$r(\Delta t) = \sum_{m=0}^{k-1} \mathrm{d}r(t_{j+m+1}, t_{j+m}) \quad (13)$$

where

$$\mathrm{d}r(t_{j+m+1}, t_{j+m}) = \gamma \times \sqrt{\left[\mathrm{d}x(t_{j+m+1})^2 + \mathrm{d}y(t_{j+m+1})^2 \right]}$$

with $\mathrm{d}x(t_{j+m+1}) = x(t_{j+m+1}) - x(t_{j+m})$ and $\mathrm{d}y(t_{j+m+1}) = y(t_{j+m+1}) - y(t_{j+m})$, where γ is $+1$ for the forward movement and -1 for the backward movement along a smooth trajectory. The direction of the movement between t_{j+m+1} and t_{j+m} was determined by examining the sign of the scaler product of two vectors: one connecting the two positions at t_{j+m} and t_{j+m+1}, and another from the position at t_{j+m} and the position a few (usually eight) data points ahead or behind along a trajectory. Note that the sampling interval for digitizing the position is set so that γ is mostly positive. The distance thus calculated with Eq. 13 gives the contour length along a trajectory for a time interval Δt, and will be referred to as the summed distance. The second method can be applied to curved, as well as linear, trajectories, unlike the first method.

2.6. Calculation of the mean-square deviation of displacement from the average within individual single trajectories of biased random walks

The mean-square displacement deviation from the average was calculated by

$$F_r^2 = \langle \left[r(\Delta t) - \langle r(\Delta t) \rangle \right]^2 \rangle$$

$$= \langle r(\Delta t)^2 \rangle - \langle r(\Delta t) \rangle^2 \quad (14)$$

$$= 2 D_{\mathrm{m}} \Delta t \quad (15)$$

where $r(\Delta t)$ is given by either Eq. 12 or Eq. 13. Here the average was taken over all the data positions (N) of a single trajectory, that is, $j = 0$ to [$N - 1 - \Delta t$/(unit sampling interval)]. Operationally, we took (i) a set of calipers set for a fixed time duration ($\Delta t = n \times$ sampling interval, $n = 1, 2, 3...$), and (ii) moved the beginning point sequentially from $j = 0$ to $j = 1$ and so on, (iii) calculating the $r(\Delta t)$ and its squares for each value of t_j, and averaging all of the calculated quantities to obtain Eq. 14. Eq. 15 then yields the motional diffusion coefficient, D_{m}.

All computer simulations and analyses were carried out on an EPSON microcomputer with an Intel 486DX2 processor using custom software written with C + +.

3. Results

Before describing the simulation results, we first theoretically consider the contribution of measurement errors in the calculation of the mean-square deviation of the sliding displacement from the average within a single noisy linear trajectory. Suppose a particle which moves with an average velocity $\langle v \rangle$ along a linear line parallel to the x-axis in a plane. The digitization of the particle position introduces two-dimensional measurement errors. The x- and y-axis components of the errors will be referred to as ϵ_x and ϵ_y. We assume that $\langle \epsilon_x \rangle = 0$ and $\langle \epsilon_y \rangle = 0$. The displacement of the particle in an interval Δt may be experimentally given by measuring the linear distance between the two end points along a linear noisy trajectory (see Eq. 12). The theoretical expression of the corresponding distance is given by

$$r(\Delta t) = \sqrt{\left\{ \left[x(\Delta t) + \epsilon_x \right]^2 + \epsilon_y^2 \right\}} \quad (16)$$

where $x(\Delta t)$ is the true distance the particle moved. Since $x(\Delta t)$, ϵ_x and ϵ_y are independent, the mean-square deviation of the sliding displacement from the average is given by

$$F_r^2(\Delta t) = \langle [r(\Delta t) - \langle v \rangle \Delta t]^2 \rangle$$
$$= (\partial r/\partial x)^2 \sigma_x^2 + (\partial r/\partial \epsilon_x)^2 \sigma_{\epsilon x}^2 + (\partial r/\partial \epsilon_y)^2 \sigma_{\epsilon y}^2$$
$$= (\partial r/\partial x)^2 2D_m \Delta t + (\partial r/\partial \epsilon_x)^2 \sigma_{\epsilon x}^2 + (\partial r/\partial \epsilon_y)^2 \sigma_{\epsilon y}^2 \quad (17)$$

with

$$(\partial r/\partial x)^2 = [x(\Delta t) + \epsilon_x]^2 / \left\{ [x(\Delta t) + \epsilon_x]^2 + \epsilon_y^2 \right\}$$

$$(\partial r/\partial \epsilon_x)^2 = [x(\Delta t) + \epsilon_x]^2 / \left\{ [x(\Delta t) + \epsilon_x]^2 + \epsilon_y^2 \right\}$$

and

$$(\partial r/\partial \epsilon_y)^2 = (\epsilon_y)^2 / \left\{ [x(\Delta t) + \epsilon_x]^2 + \epsilon_y^2 \right\}$$

where we used

$$\sigma_x^2 = \langle [x(\Delta t) - \langle v \rangle \Delta t]^2 \rangle = 2D_m \Delta t$$

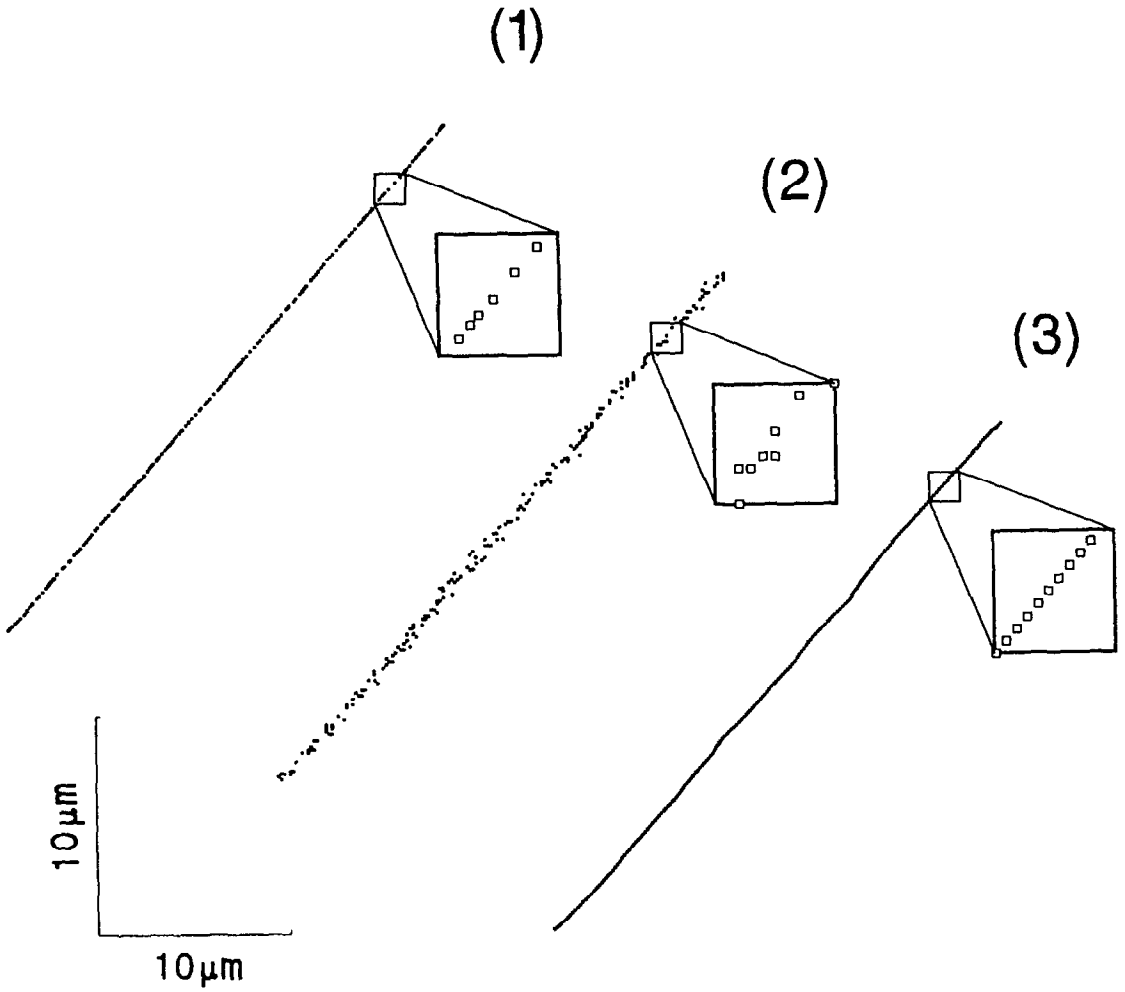

Fig. 1. Examples of linear trajectories of simulated biased random walks. (1) portion of a noise-free trajectory of 4096 data points, which were generated with a given motional diffusion coefficient of 1×10^{-9} cm^2/s and a given drift velocity of 5×10^{-4} cm/s and with a sampling interval of 1/30 s, as described in Section 2; (2) portion of a trajectory with digitization noise added to the positional data points in the entire segment of the trajectory (1) as described in Section 2; (3) portion of a trajectory obtained after smoothing the noisy trajectory (2) by low-pass filtering at a cut-off frequency of 3 Hz as described in the text.

and $\sigma_{\epsilon x}^2$ and $\sigma_{\epsilon y}^2$ are the variances of ϵ_x and ϵ_y [12]. If $|x(\Delta t) + \epsilon_x| \gg \epsilon_y$, Eq. 17 is reduced to

$$F_r^2(\Delta t) = 2D_m \Delta t + \sigma_{\epsilon x}^2 \quad (18)$$

In other words, the mean-square deviation of the sliding distance from the average increases linearly with the time interval when the interval is relatively large (above the variance of the total measurement errors). We may then be able to evaluate a motional diffusion coefficient from a single linear noisy trajectory without smoothing, although this depends on the length of trajectories as will be shown below. When a noisy trajectory is curved, in contrast, it is difficult to obtain the precise sliding distance along the trajectory without smoothing, and thus difficult to evaluate the motional diffusion coefficient.

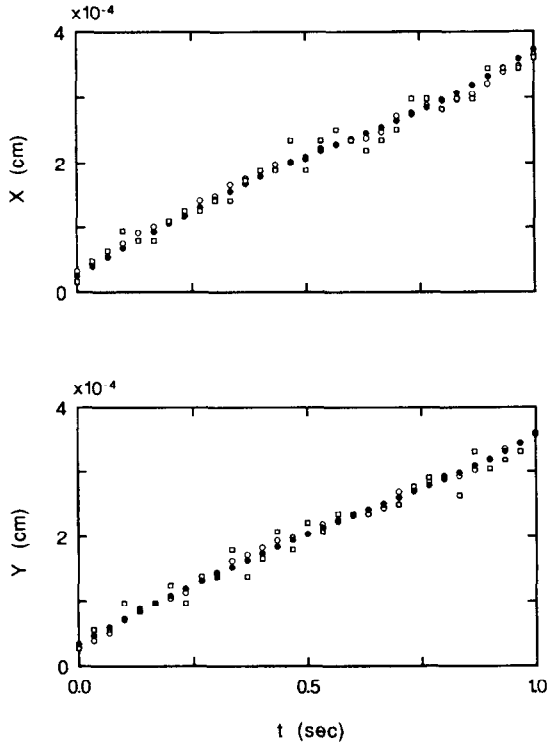

Fig. 2. x- (upper panel) and y-coordinates (lower panel) of the positional data points in the linear trajectories shown in Fig. 1 as a function of time. Open circles: coordinates of the noise-free trajectory (1) in Fig. 1; open squares: coordinates of the noisy trajectory (2) in Fig. 1; filled circles: coordinates obtained after smoothing the noisy coordinates (open squares) by low-pass filtering (see text). From the smoothed coordinates, the smoothed trajectory (3) in Fig. 1 was reconstructed.

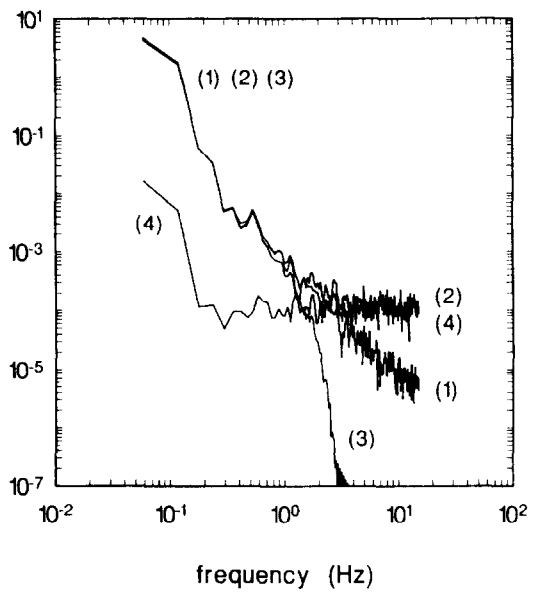

Fig. 3. The power spectra of the x-coordinate time series (with the linear trends removed) of trajectories shown in Fig. 2. A linear trend was removed with a linear line connecting the first and last points in each time series. (1) Spectrum of the noise-free coordinates (open circles in Fig. 2); (2) spectrum of the noisy coordinates (open squares in Fig. 2); (3) spectrum obtained after removing the high-frequency Fourier components of the spectrum (2) by low-pass filtering at 3 Hz; (4) spectrum of the noise alone, which was used to make the noisy coordinates (open squares in Fig. 2).

In the following we describe the simulation results. We first deal with linear trajectories and then curved trajectories. Line 1 in Fig. 1 shows a portion of a computer-generated, noise-free trajectory (see Section 2). The distances between the adjacent dots along the trajectory are not constant and are randomly varied. The trajectory was then made noisy, as described in Section 2. Line 2 in Fig. 1 shows a portion of the resulting noisy trajectory, which is very similar to a digitized trajectory of a real filament sliding movement. Considering that in the experimental digitized trajectory a smoother noise-free trajectory is buried, we thus examined some smoothing methods in order to reconstruct a smooth trajectory from a noisy trajectory without loosing the physical characteristics of the original biased random walks. We found that smoothing by low-pass filtering in frequency domain worked best for our purpose. In the following, we will hence describe the conditions for using the smoothing method.

The upper panel of Fig. 2 shows the x-coordinates of the simulated trajectories as a function of discrete time, while the lower panel shows the y-coordinates of the trajectories. In each panel of the figure, the open circles show the coordinates of the original noise-free trajectory 1 in Fig. 1, while the open squares show those of the noisy trajectory 2 in Fig. 1. (For filled circles, see below.)

The smoothing over trajectories in this study was carried out with Fourier transform techniques [11], as described in Section 2. Fig. 3 shows the FFT power spectra of x-coordinate time-series data of trajectories after linear trends were removed (see Section 2). Spectrum 1 in Fig. 3 shows that for the original noise-free trajectory, and spectrum 2 in Fig. 3 shows that for the noisy trajectory. Spectrum 4 in Fig. 3 shows that for the noise alone, which was added to the smooth trajectory to form the noisy trajectory. Spectrum 2 of the noisy trajectory is the sum of spectrum 1 of the original noise-free trajectory and

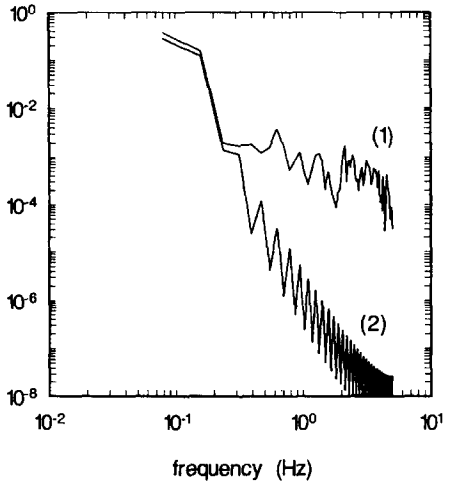

Fig. 4. The power spectra of x-coordinates of a real experimental trajectory of a microtubule induced to slide by kinesin. The position of microtubules was determined by digitizing the position of their front tip, using a mouse-driven video cursor on a computer screen. A linear trend was removed from the coordinate data as described in Fig. 3. (1) Spectrum of the original digitized trajectory; (2) spectrum obtained after removing high-frequency Fourier components in the spectrum (1) by low-pass filtering at 1/3 Hz. The appropriate cut-off frequency depends on both the sampling interval and the fluctuation of sliding movement as is described in the text. Microtubules were prepared from swine brain and kinesin was prepared from bovine brain.

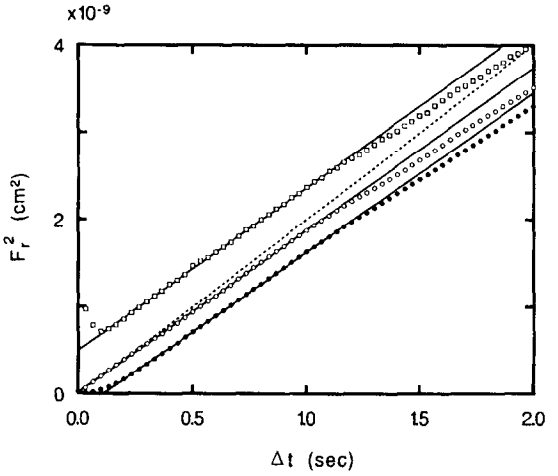

Fig. 5. The mean-square displacement deviation from the average as a function of the time interval calculated from single linear trajectories (4096 data points) as described in Section 2. Open circles: the mean-square deviation calculated within a noise-free trajectory. Filled circles: the mean-square deviation calculated within a smoothed single trajectory. The summed distances (see Eq. 13) were used for the average calculation in the above two cases. Open squares: the mean-square deviation calculated with the linear distances between the two end points (see Eq. 12) within a noisy single trajectory. The noise-free, noisy and smoothed trajectories were generated as described in Fig. 1. The solid lines indicate the linear portion of each of these three lines of the mean-square deviation, which were determined following the method of Uyeda et al. [15]. Half of the slope of each linear line gives a motional diffusion coefficient. The dotted line indicates the slope corresponding to the diffusion coefficient used for generating the trajectory on computer.

the spectrum of the noise alone 4. We removed the high-frequency Fourier components from the noisy trajectory by low-pass filtering (at 3 Hz cut-off frequency in Fig. 3). Spectrum 3 in Fig. 3 shows the resulting filtered spectrum. The filtered spectrum is similar to that of the original spectrum 1, except at high frequencies where the spectrum intensity is small. Since the frequency components with large intensities dominantly contribute to the diffusion coefficient, we can expect that low-pass filtering at an appropriate cut-off frequency does not affect the values of the diffusion coefficients significantly. The y-coordinates of trajectories produced FFT power spectra similar to those shown in Fig. 3.

For comparison, Fig. 4 shows examples of the FFT power spectra of a real trajectory of the microtubule sliding movement driven by kinesin. Spec-

trum 1 represents that for the original digitized trajectory, while spectrum 2 that for the smoothed trajectory. Note that the power spectra of the real trajectory before and after the low-pass filtering are similar to those made by simulation.

The x- and y-coordinates of noisy trajectories generated by simulation were first separately low-pass filtered in a frequency domain, and then the remaining Fourier components were separately transformed back by IFFT as described above, to smooth over the x- and y-coordinate time-series data. The filled circles in Fig. 2 show examples of the smoothed coordinates. The smoothed x- and y-coordinates generated smooth trajectories as shown by line 3 in Fig. 1. Although the distances between the adjacent dots in the smoothed trajectory (line 3 in Fig. 1) are less random than those in the original trajectory (line 1 in Fig. 1), fluctuations intrinsic to the original biased random motions are preserved even after smoothing as will be shown below.

We calculated the mean-square displacement deviation from the average within a noise-free single trajectory (consisting of 4096 data points) as described in Section 2, a segment of which is shown by the line 1 in Fig. 1. For the calculation we used the summed distance (see Eq. 13). The mean-square deviation is shown as a function of time interval in Fig. 5 (open circles). The initial part of the line is almost linear as indicated by the filled line, half of the slope of which yields a motional diffusion coefficient. The motional diffusion coefficient determined from the slope is close to that used for generating the biased random walk on computer, which corresponds to the dotted line in Fig. 5. We also calculated the mean-square deviation of displacement from the average within a smoothed single trajectory, a segment of which is shown by line 3 in Fig. 1. For the calculation, we used the summed distance (see Eq. 13). The calculated mean-square deviation is shown by the filled circlers in Fig. 5. There is a lag in the

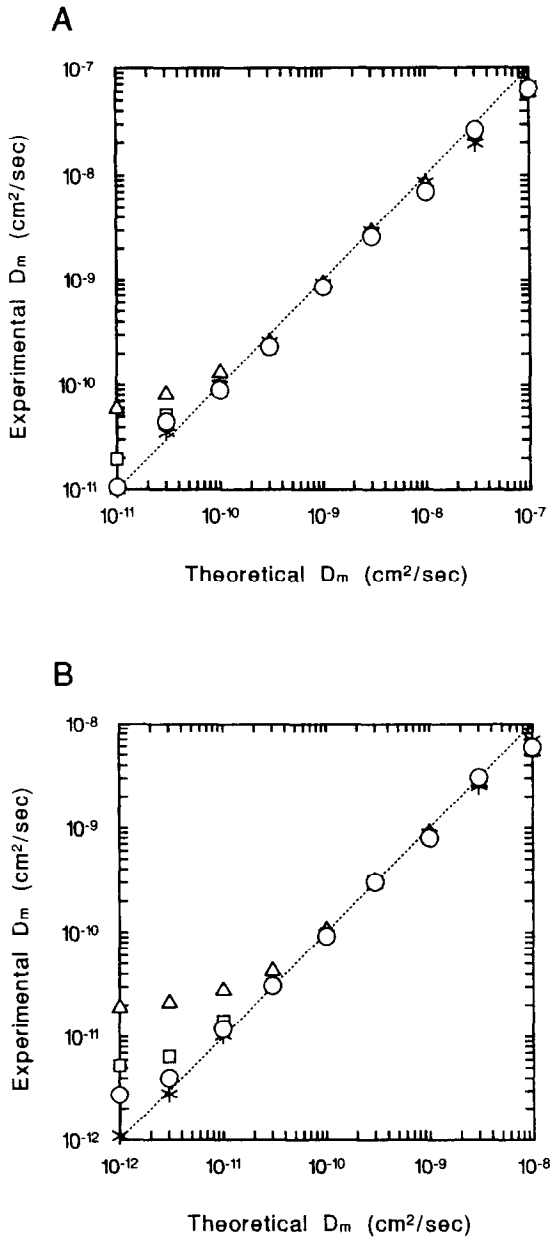

Fig. 6. (A) The motional diffusion coefficients evaluated from single linear trajectories versus theoretical motional diffusion coefficients used for generating trajectories on computer with a given drift velocity of 5×10^{-4} cm/s and with a sampling interval of 1/30 s (4096 data points). Symbols: (*) the diffusion coefficients evaluated from original noise-free trajectories; others: the diffusion coefficients evaluated from (noisy) trajectories smoothed by low-pass filtering at (△) 3, (□) 1.5 and (○) 1 Hz. (B) the same as in A except for the given drift velocity of 1×10^{-4} cm/s and the sampling interval of 1/10 s. Symbols: (*) diffusion coefficients obtained from original noise-free trajectories; others: diffusion coefficients obtained from (noisy) trajectories smoothed by low-pass filtering at (△) 1, (□) 0.5 and (○) 1/3 Hz. Each symbol shows the result of a single simulation experiment.

line of the filled circles, but the initial linear portion of the line (shown by the filled line) after the lag is almost parallel to that of the line for open symbols, showing that the linear portion of the line after the lag gives the correct motional diffusion coefficient. The lag in the line of the closed circles is a result of the smoothing by low-pass filtering.

So far, the mean-square displacement deviation from the average was calculated by using the summed distances of Eq. 13. For comparison, we repeated the same calculation with the linear distances between the two end points (Eq. 12) obtained from the single trajectory. The results are shown by the open squares in Fig. 5. For the time interval > ca. 0.1 s, the line increases almost linearly with time up to ca. 1 s, as do the other two lines. The line of the open squares is consistent with Eq. 18. The slope of this linear line is the same as that of the other two lines, indicating that the open square line gives the same value for the motional diffusion coefficient as do the other two lines. The intercept on the ordinate of the line of open squares is close to the square of the measurement errors given in the simulation, as is expected from Eq. 18.

The readers may think that the use of the linear distance between the two end points along a linear noisy trajectory works successfully for the calculation of the mean-square deviation of displacement from the average and, therefore, smoothing is not necessary. However, this is only the case when the length of a single trajectory is sufficiently large. When the length of a single trajectory is as small as consisting of 200 positional data points, as obtained in real experiments under standard conditions, the use of the linear distance between the two end points does not work and the use of smoothing together with the summed distance is necessary, as will be shown below. Thus in the following, we mainly describe the results obtained with the summed distance of Eq. 13.

The breakdown in linearity at a long time interval, which is expected to ultimately occur in graphs such as in Fig. 5, is not due to the vanished correlation, but due to the increase in statistical errors. Since the data number in a set of calipers for the average calculation (see Section 2) is larger for a longer time interval, the number of independent data available from a single trajectory is smaller, and thus the statistical errors increase over a longer time interval [8,13]. It is interesting to note that the minor wavy structure of the open symbol line is nonetheless preserved even in the other two lines.

We calculated the average displacement of a particle along a single either noise-free or smoothed noisy trajectory as a function of time interval with Eqs. 5 and 12 (see Section 2), and found that these two lines were linear and had the same slope (data not shown). Since the slope of these lines gives the drift velocity, this finding shows that the drift velocity obtained from the noise-free trajectory is the same as that obtained from the smoothed noisy trajectory. The drift velocity obtained from these trajectories was also the same as the drift velocity value given for the generation of the original trajectory on computer.

We systematically studied the effects of smoothing on the motional diffusion coefficients determined from individual trajectories, at various diffusion coefficients and drift velocities. To do so, from either single noise-free or smoothed noisy trajectories we obtained "experimental" motional diffusion coeffi-

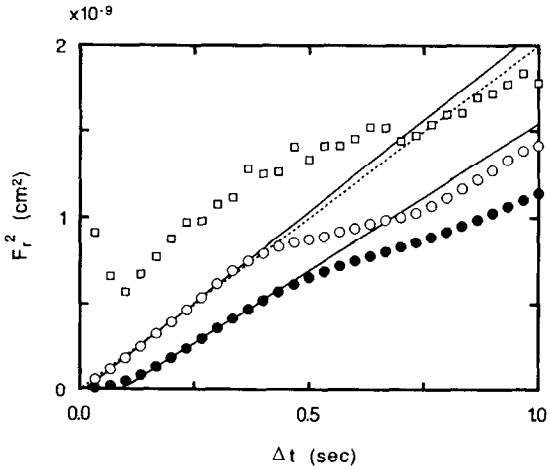

Fig. 7. The mean-square displacement deviation from the average as a function of the time interval calculated from single linear trajectories (200 data points) as described in Section 2. Other conditions and symbols are the same as in Fig. 5. The solid lines indicate the linear portion of the two lines of open and filled circles, which were determined following the method of Uyeda et al. [15]. Half of the slope of each linear line gives a motional diffusion coefficient. The dotted line indicates the slope corresponding to the diffusion coefficient used for generating the trajectory on computer.

cients, and compared them with the given (theoretical) values of the coefficients for generating trajectories. A set of the results is shown in Fig. 6A. Another set of the results is shown in Fig. 6B. The trajectories (consisting of 4096 data points) used for the analyses in Fig. 6A were generated with a given drift velocity of 5×10^{-4} cm/s, which corresponded to the velocity of actin filaments on skeletal muscle heavy meromyosin or that of microtubule on sea urchin dynein, and with the sampling interval of 1/30 s. The trajectories (4096 data points) used for the analyses in Fig. 6B were generated with a given drift velocity of 1×10^{-4} cm/s, which corresponded to the velocity of microtubule on bovine brain kinesin, and with a sampling interval of 1/10 s.

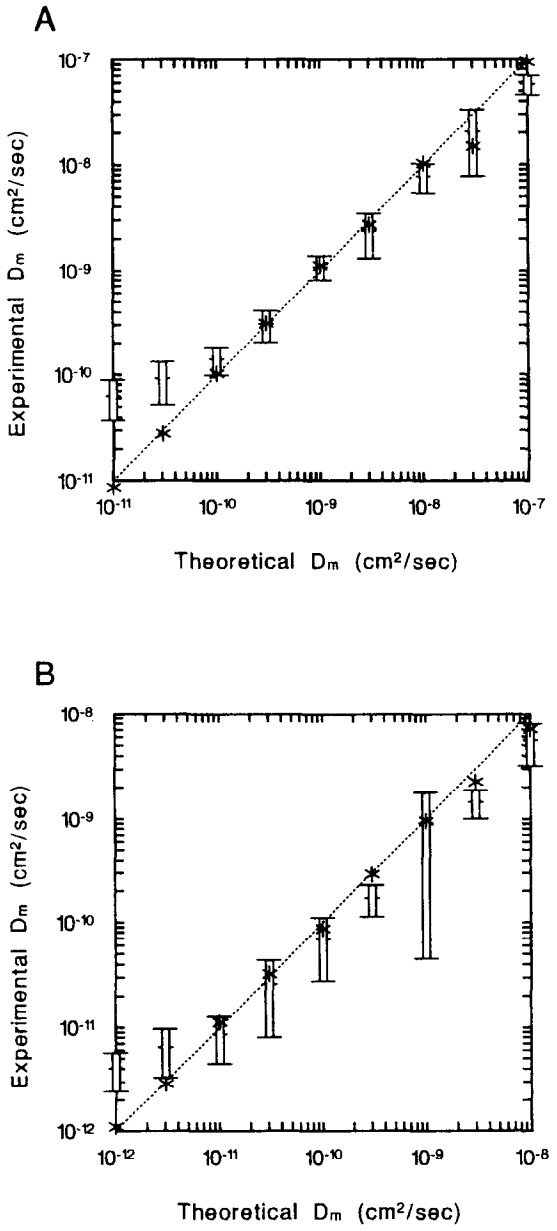

In Fig. 6A and B, motional diffusion coefficients obtained from noise-free trajectories (stars in both figures) were almost the same as the theoretical diffusion coefficients over the entire range of diffusion coefficients studied. When the noisy trajectories were smoothed by low-pass filtering at 1 Hz cut-off frequency in Fig. 6A (circles), they yielded correct diffusion coefficients over the entire range studied. The appropriate cut-off frequency for low-pass filtering is primarily proportional to the inverse of the sampling interval (Δ), or the Nyquist critical frequency [$= 1/(2\Delta)$]. For example, if we repeat the same simulation as shown in Fig. 6A with a sampling interval of 1/10 instead of 1/30 s, we have to reduce the cut-off frequencies for low-pass filtering by a factor of 1/3 to get the same effect. In Fig. 6B, filtering at 1/3 Hz cut-off frequency (circles) yielded correct diffusion coefficients in the range of 0.3×10^{-11} and 0.3×10^{-8} cm^2/s.

We next examined the dependence on the number of data points. So far we studied trajectories consisting of 4096 data points. We reduced the data number down to 200 data points, and then repeated similar analyses. Fig. 7 shows the mean-square displacement deviation from the average, which was calculated

Fig. 8. (A) The motional diffusion coefficients evaluated from single linear trajectories versus theoretical motional diffusion coefficients used for generating trajectories on computer with a given drift velocity of 5×10^{-4} cm/s and with a sampling interval of 1/30 s (200 data points). Symbols: (*) the diffusion coefficients evaluated from original noise-free trajectories; open bars: the diffusion coefficients evaluated from single noisy trajectories smoothed by low-pass filtering at 3 Hz. (B) the same as in A except for the given drift velocity of 1×10^{-4} cm/s, the sampling interval of 1/10 s and the low-pass filtering at 1/3 Hz. The summed distance (see Eq. 13) was used in the average calculation for the D_m evaluation. The open bars show the mean $\pm$ S.D. ($n = 5$ different trajectories); the S.D. for the asterisks was slightly larger than the size of the symbols.

from either a single noise-free (open circles) or smoothed noisy (filled circles) trajectory of 200 data points. In the calculation we used the summed distance (Eq. 13). The mean-square deviation of displacement from the average as a function of time interval calculated within the smoothed trajectory is similar to that within the original trajectory except for the presence of a lag in the former curve. The initial portion of these curves (after the lag for closed circles) is linear, although the linear range is smaller than that in Fig. 5. Half of the slope of the initial linear portion (indicated by a filled line) of open circle curves gives a diffusion coefficient, which is close to the theoretical value (indicated by the dotted line) used for generating the trajectory. Half of the initial slope of the filled circle curve after the lag gives a diffusion coefficient, which is close to, but in this case slightly smaller than, the theoretical value. The open squares in Fig. 7 show the mean-square deviation of displacement from the average calculated with the linear distances between the two end points obtained from the unsmoothed noisy trajectory. In this case, it is difficult to identify the linear portion of the open square data line when it only exists alone, and it is thus not possible to apply Eq. 18 for the D_m evaluation.

We generated trajectories consisting of 200 data points with various given diffusion coefficients and at two different drift velocities, then added digitized noise to them and then later smoothed them over. From either single noise-free or smoothed noisy trajectories, we evaluated diffusion coefficients and compared them with the theoretical values. The results are summarized in Fig. 8A and B. In Fig. 8A,

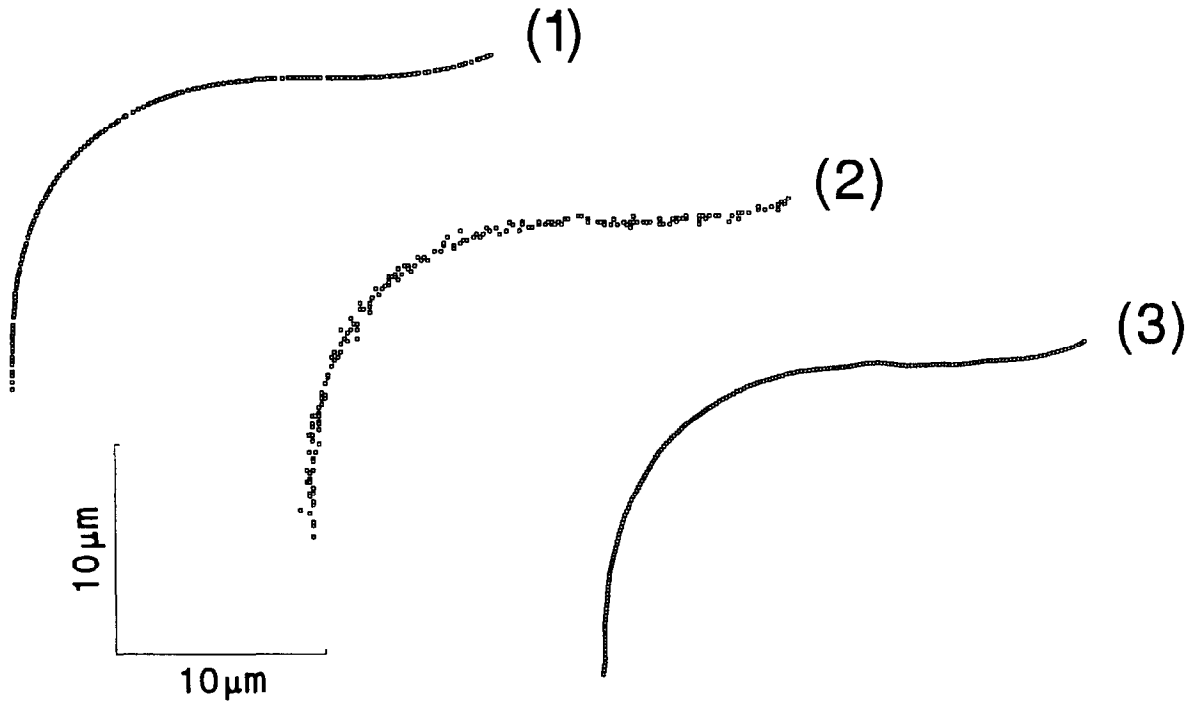

Fig. 9. Examples of curved trajectories of simulated biased random walks. (1) A trajectory of 200 data points generated with a given motional diffusion coefficient of 1×10^{-9} cm^2/s, a given drift velocity of 5×10^{-4} cm/s and a sampling interval of 1/30 s as described in Section 2; (2) a noisy trajectory (see Section 2); (3) a smoothed trajectory (low-pass filtered at 3 Hz; see Section 2). The function used for curving trajectories is

$$\theta(t_j) = \pi \times \sin^2\left[20\pi \sum_{i=1}^{j} \mathrm{d}r(t_i)\right]/2$$

(see Section 2) where the unit for $\mathrm{d}r(t_i)$ is cm.

the trajectories were generated with a given drift velocity of 5×10^{-4} cm/s and a sampling interval of 1/30 s. Those in Fig. 8B were generated with another drift velocity of 1×10^{-4} cm/s and a sampling interval of 1/10 s. In Fig. 8A, noisy trajectories when filtered at 3 Hz cut-off frequency gave correct diffusion coefficients in the range of the coefficients between 1×10^{-10} and 0.3×10^{-7} cm^2/s. In Fig. 8B, filtering at the 1/3 Hz cut-off frequency was required to get correct diffusion coefficients in the range between 1×10^{-11} and 1×10^{-9} cm^2/s, although the values in this range appear to be consistently underestimated. When the diffusion coefficients are not within these limits, it is not possible to obtain correct motional diffusion coefficients from single trajectories even after filtering. However, the actual experimental values of motional diffusion coefficients of actin filaments sliding over skeletal muscle heavy myosin as well as of microtubules sliding over sea urchin dynein are about 10^{-9} cm^2/s, while those of microtubules sliding over kinesin are larger than 10^{-11} cm^2/s and smaller than 10^{-9} cm^2/s, as shown by our preliminary experiments. The number of data points in a real experimental trajectory is about 200. Therefore, our method for evaluating motional diffusion coefficients from single trajectories can be practically applied to real experimental data of the above-mentioned actin and microtubule sliding movements.

We next examined the effect of curvature of trajectories on the determination of diffusion coefficients within single trajectories after smoothing. We generated curved trajectories (consisting of 200 data points) with various given diffusion coefficients and a given drift velocity of 5×10^{-4} cm/s. Examples of such curved trajectories are shown in Fig. 9. From such single curved trajectories, we evaluated diffusion coefficients and compared them with theoretical values. The results are summarized in Fig. 10, which are similar to those in Fig. 8A. Thus, even from curved single trajectories consisting of 200 data points, it is possible to obtain almost correct motional diffusion coefficients in the range between 1×10^{-10} and 1×10^{-7} cm^2/s after smoothing for the sliding movements of actin/heavy meromyosin and microtubule/dynein.

Finally we applied our smoothing method to a real experimental trajectory of a 6.4 μm microtubule

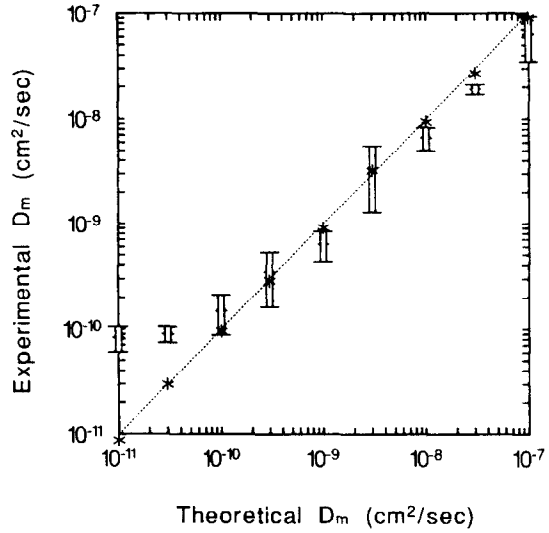

Fig. 10. The motional diffusion coefficients evaluated from single curved trajectories versus the theoretical motional diffusion coefficients used for generating trajectories on computer with a given drift velocity of 5×10^{-4} cm/s and with a sampling interval of 1/30 s (200 data points). Symbols: (*) the diffusion coefficients evaluated from original single noise-free trajectories; open bars: the diffusion coefficients evaluated from single (noisy) trajectories smoothed by low-pass filtering at 3 Hz. The open bars show the mean ± S.D. ($n = 5$ different trajectories). The S.D. for the asterisks was slightly larger than the size of the symbols.

sliding over dynein, which is shown in the inset of Fig. 11. The trajectory is curved. We smoothed the entire trajectory and calculated the mean-square deviation of displacement from the average by using the summed distances obtained from the single trajectory. The result is shown by the filled circles in Fig. 11. Half of the slope of the linear line yielded a value of 1.0×10^{-9} cm^2/s for the motional diffusion coefficient of the filament. To check whether the value is reasonable, we calculated the mean-square deviation of displacement from the average by averaging the sliding distances over five different linear unsmoothed trajectories of five different microtubules in the length range of 5.0–8.0 μm (with an average of 5.4 μm), and obtained a value of $(0.8 \pm 0.1) \times 10^{-9}$ (mean ± s.d.) cm^2/s for the motional diffusion coefficient. The value obtained from a single smoothed trajectory is close to the value obtained by the conventional averaging method, and therefore substantiates our method for evaluating the motional diffusion coefficient of individual fila-

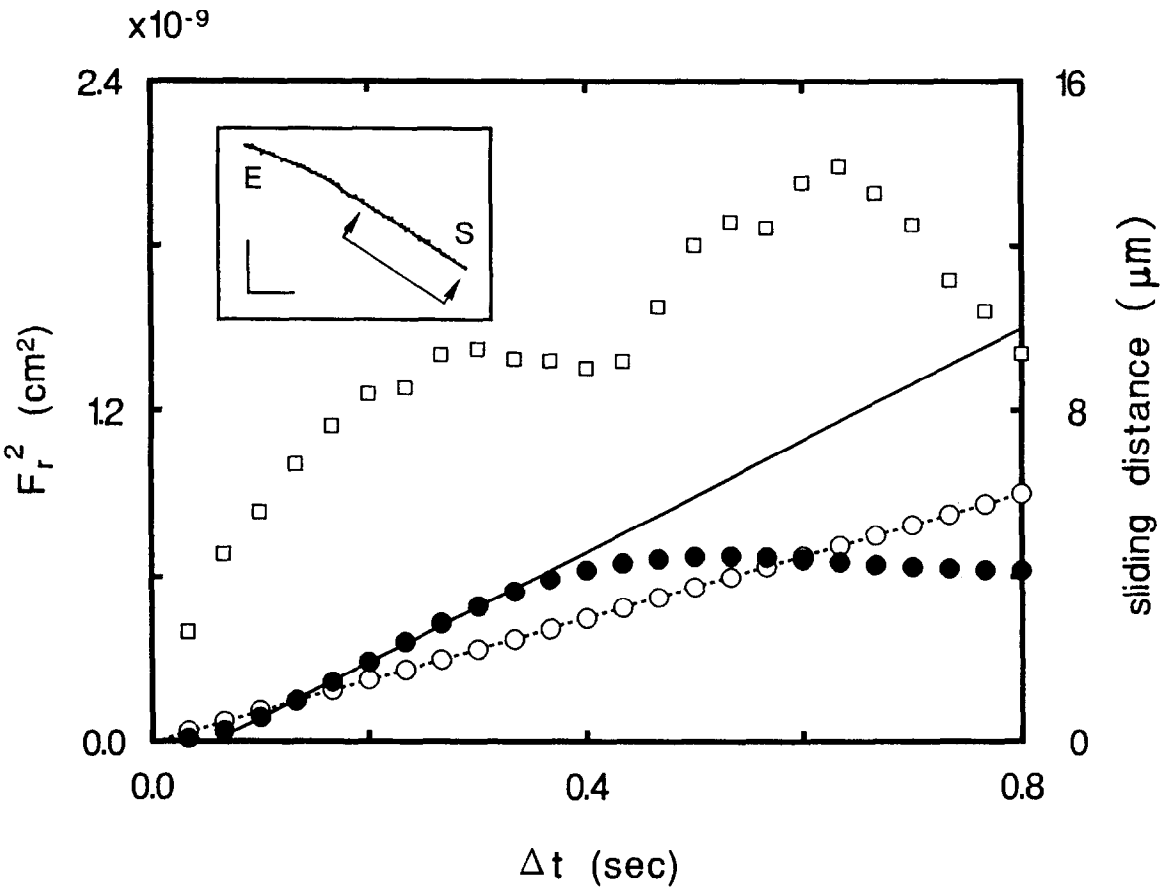

Fig. 11. The mean-square displacement deviation from the average as a function of the time interval, evaluated from a single trajectory obtained in a real in vitro motility experiment with a 6.4-μm microtubule sliding over dynein on a glass surface. Dynein was prepared from sea urchin sperm. The microtubule position was determined as described in Fig. 4. (●) Mean-square deviation calculated with the summed distances (Eq. 13) obtained from the entire segment of the curved trajectory shown in the inset (110 data points) after smoothing at 1/3 Hz. The solid lines indicate the linear portion of the closed circle line, which was determined following the method of Uyeda et al. [15]. Half of the slope yields a value of 1.0×10^{-9} cm^2/s for D_m. (○) Sliding distance as a function of time interval, evaluated by using the summed distances obtained from the entire smoothed trajectory shown in the inset. The dotted line is a linear regression line, yielding a value of 7.6 μm/s for the sliding speed. (□) Mean-square deviation calculated with the linear distances between the two end points (Eq. 12) within the linear portion of the trajectory (60 data points) indicated by the line with two arrows in the inset. S and E: the start and the end of the sliding. Scales: 5 μm.

ments. It should be pointed out that the value of the motional diffusion coefficient is less than 1/5 of the longitudinal diffusion coefficient of a microtubule with the same length freely suspended in solution. A similar smaller value has been observed with the diffusion coefficient of microtubules in the Brownian movement over dynein in the presence of ADP and vanadate [6]. Note also that the average sliding distance (open circles) linearly increases with time, yielding a value of 7.6 μm/s for the average sliding speed.

With the positional data available from a linear portion of the unsmoothed trajectory (indicated by a linear line with two arrows in the inset), we calculated the mean-square deviation of displacement from the average by using the linear distances between the two end points along the trajectory. The results are shown by the open squares in Fig. 11. Since there is

no apparent linear portion in the plot in this case, it is very difficult to apply Eq. 18 to obtain the motional diffusion coefficient.

4. Conclusions

In this paper we have defined the conditions of a method for smoothing noisy trajectories in the in vitro sliding motion so that the mean-square displacement deviation from the average can be calculated within the single curved, as well as linear trajectories of individual sliding filaments. The mean-square deviation within a single trajectory thus yields the motional diffusion coefficient of individual filaments. Hence, the present method is useful, in particular, when the length dependence of the diffusion coefficients of sliding filaments is analyzed. The present smoothing method uses low-pass filtering in the frequency domain. Low-pass filtering to smooth sliding trajectories has previously been used by others. For example, Sheetz et al. [14] used it for smoothing to obtain the average sliding speed. As shown here, smoothing by low-pass filtering at an appropriate cut-off frequency does not affect even the fluctuation characteristics intrinsic to the in vitro sliding motion.

There are, however, some limitations in the application of the present method. The method works only for sliding motions having motional diffusion coefficients within a limited range. As was mentioned in this paper, the motional diffusion coefficients of actin sliding over skeletal muscle myosin and of microtubules sliding over either sea urchin dynein or bovine brain kinesin are within these limits. When the method is used for other systems, therefore, some simulation studies under particular experimental conditions should be done first before applying it to experimental data.

Acknowledgements

This work was supported by a Grant-in-Aid on the Priority Area of Molecular Mechanism of Biological Sliding Movement (No. 015670002) and in part by a Grant for Joint Research on the in vitro sliding movement, from the Ministry of Education, Science and Culture of Japan.

References

[1] S.J. Kron and J.A. Spudich, Proc. Natl. Acad. Sci. USA, 83 (1986) 6272.
[2] R.D. Vale, T.S. Reese and M.P. Sheetz, Cell, 42 (1985) 39.
[3] B.M. Paschal, H.S. Shpetner and R.B. Vallee, J. Cell Biol., 105 (1987) 1273.
[4] K. Tawada and K. Sekimoto, Biophys. J., 59 (1991) 343.
[5] K. Tawada and K. Sekimoto, J. Theor. Biol., 150 (1991) 193.
[6] R.D. Vale, D.R. Soll and I.R. Gibbons, Cell, 59 (1989) 915.
[7] N.G. van Kampen, Stochastic Processes in Physics and Chemistry, North Holland, Amsterdam, 1981.
[8] H. Qian, M.P. Sheetz and E.L. Elson, Biophys. J., 60 (1991) 910.
[9] H.C. Berg, Random Walks in Biology, Expanded Edition, Princeton University Press, Princeton, NJ, 1993.
[10] H. Gould and J. Tobochnik, An Introduction to Computer Simulation Methods, Part 2, Addison–Wesley, Reading, MA, 1988.
[11] W.H. Press, B.P. Flannery, S.A. Teukolsky and W.T. Vetterling. Numerical Recipes in Pascal, Cambridge University Press, Cambridge, MA, 1989.
[12] P.R. Bevington and D.K. Robinson, Data Reduction and Error Analysis for the Physical Sciences, McGraw-Hill, New York, 2nd edn., 1992.
[13] G.M. Lee, A. Ishihara and K.A. Jacobson, Proc. Natl. Acad. Sci. USA, 88 (1991) 6274.
[14] M.P. Sheetz, S.M. Block and J.A. Spudich, in R.B. Vallee (Ed.), Methods in Enzymology, Vol.134, Academic Press, San Diego, CA, 1986, p. 531.
[15] T.Q.P. Uyeda, H.M. Warrick, S.J. Kron and J.A. Spudich, Nature (London), 352 (1991) 307.